



# LUND UNIVERSITY

## Wenlock metabentonites from Gotland, Sweden: geochemistry, sources and potential as chemostratigraphic markers

Batchelor, R.A.; Jeppsson, Lennart

*Published in:*  
Geological Magazine

*DOI:*  
[10.1017/S001675689900285X](https://doi.org/10.1017/S001675689900285X)

1999

[Link to publication](#)

*Citation for published version (APA):*

Batchelor, R. A., & Jeppsson, L. (1999). Wenlock metabentonites from Gotland, Sweden: geochemistry, sources and potential as chemostratigraphic markers. *Geological Magazine*, 136(6), 661-669.  
<https://doi.org/10.1017/S001675689900285X>

*Total number of authors:*  
2

### General rights

Unless other specific re-use rights are stated the following general rights apply:  
Copyright and moral rights for the publications made accessible in the public portal are retained by the authors and/or other copyright owners and it is a condition of accessing publications that users recognise and abide by the legal requirements associated with these rights.

- Users may download and print one copy of any publication from the public portal for the purpose of private study or research.
- You may not further distribute the material or use it for any profit-making activity or commercial gain
- You may freely distribute the URL identifying the publication in the public portal

Read more about Creative commons licenses: <https://creativecommons.org/licenses/>

### Take down policy

If you believe that this document breaches copyright please contact us providing details, and we will remove access to the work immediately and investigate your claim.

LUND UNIVERSITY

PO Box 117  
221 00 Lund  
+46 46-222 00 00

# Wenlock metabentonites from Gotland, Sweden: geochemistry, sources and potential as chemostratigraphic markers

R. A. BATCHELOR\* & L. JEPPSSON†

\*School of Geography and Geosciences, University of St Andrews, North Haugh, St Andrews, Fife KY16 9ST, UK

†Department of Geology, Division of Historical Geology and Paleontology, Sölvegatan 13, S-223 62 Lund, Sweden

(Received 11 November 1998; accepted 20 April 1999)

**Abstract** – Two metabentonite suites occur within the Wenlock limestones and marls of Gotland, one within the Slite Formation (*M. belophorus* to the *C. ellesae* biozones) and the other in the Mulde Formation (*G. nassa*–*M. dubius* Biozone). Their geochemical characteristics based on rare-earth element (REE) distributions in apatite crystals separated from the metabentonites suggest origins from three separate volcanic sources. One of these sources has an alkaline affinity, reflected in relatively high levels of Th, Nb and Zr, which suggests that it may have lain over thickening continental crust during the waning stages of the closure of the Tornquist Sea, while the other two represent calc-alkaline magmas. The source of the volcanic ash is placed some 400 km to the southwest of Gotland, on the Tornquist–Teyseyre Zone, which is the northernmost expression of the Trans-European Suture Zone. Distinctive differences in REE distribution in apatite from these metabentonites should assist in future correlation studies in Wenlock stratigraphy, both within the Baltic region and further afield.

## 1. Introduction

Correlation across faunal provinces the biostratigraphy of which has been determined using different faunas (e.g. conodont or graptolites) remains a problem for a detailed understanding of depositional and tectonic histories. If a unique chronostratigraphic plane could be identified within the lithological successions, it would revolutionize stratigraphic correlation and provide a valuable tool for high-resolution stratigraphy.

Within the Silurian of northern Europe, there exist numerous clay bands identified as K-bentonites (Fortey, Merriman & Huff, 1996). On Gotland, Sweden, bentonites have been identified throughout the Silurian succession (Laufeld & Jeppsson, 1976), and a detailed geochemical study of two Llandovery examples (Batchelor & Jeppsson, 1994) provided chemical fingerprints for future correlation work.

This work focusses on a suite of metabentonites from the Wenlock of Gotland, and provides detailed geochemical fingerprints based on rare-earth element (REE) and other elements within euhedral apatite microphenocrysts that occur as ubiquitous volcanogenic accessory minerals in the metabentonites. Such information will allow comparisons to be made with other Wenlock metabentonites in northern Europe, and forms part of a wider programme on the geochemical characterization of Silurian metabentonites.

### 1.a. Biostratigraphy

The island of Gotland in the Baltic Sea is composed mostly of limestones and marls of Wenlock and

Ludlow age. A narrow strip of Upper Llandovery rocks is exposed along the northwest coast of the island (Fig. 1). The geology of Gotland has been described by Hede (1960), and a more detailed account of field localities has been compiled by Laufeld (1974) and Jeppsson & Jerre (unpub. data), whose terminology is used in this work. The new latest Telychian–early Homerian standard zonation, based on conodont biostratigraphy, provides a resolution similar to that of the graptolite zonation (Jeppsson, 1997b).

The Wenlock Series on Gotland is divided into eight formations: Lower Visby (upper part only), Upper Visby, Högklint, Tofta, Slite, Halla, Mulde and Klinteberg in ascending stratigraphical order. The Slite and Mulde formations are characterized by the occurrence of putative volcanogenic clays (Fig. 2). These clays are characterized by their sharp upper and lower contacts with their host lithology. The Slite limestone quarries (Slitebrottet 1 and 2, and Filehajdar 1) afford excellent exposure and a sequential suite of seven clays was sampled there.

The oldest sample (SW26), the Y clay bed from Slitebrottet 2, was deposited during the middle *K. walliseri* Biozone (though the number of conodonts available is too low definitely to rule out the lowermost *K. patula* Biozone), equivalent to the topmost *Monograptus belophorus* Biozone or lowermost *Cyrtograptus rigidus* Biozone. This coincides with the Sanda Primo Episode as defined by Jeppsson, Aldridge & Dorning (1995). The next five Slite clays (samples SW42–SW29) occur within the Allekvia Primo Episode, which is represented by 31 m of argillaceous limestone (Jeppsson, Aldridge & Dorning, 1995). Biostratigraphically, this episode is

\* Author for correspondence: rab@st-andrews.ac.uk

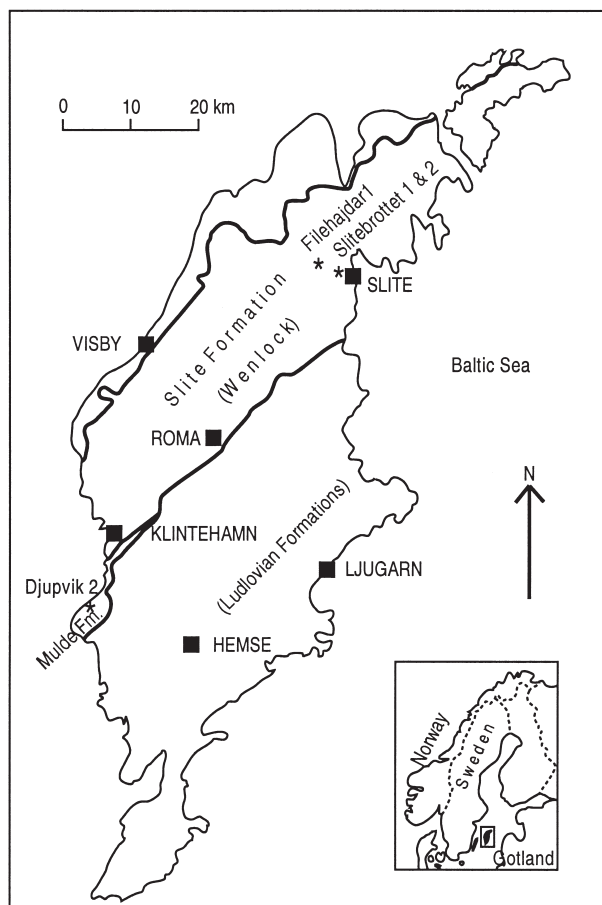


Figure 1. Sketch map of Gotland showing the boundaries of the Slite and Mulde formations (after Hede, 1960) and sampling localities.

coeval with the *Kockeella ortus ortus* and *Cyrtograptus ellesae* biozones within the Sheinwoodian Stage. The youngest sampled Slite clay bed (sample SW49 from Filehajdar 1) is very close to the Sheinwoodian–Homerian boundary. The *O. s. sagitta* Biozone has not been found in Filehajdar, and the eponymous biozonal species is very rare on Gotland, but other evidence indicates that this clay is found in the lowermost part of that zone (Jeppsson, 1997b). The base of the *O. s. sagitta* Biozone is coeval with or close to the base of the *C. lundgreni* Biozone, suggesting that this clay was deposited during the Valleviken Event (Jeppsson, Aldridge & Dorning, 1995).

Another succession of five clays from the Mulde Formation was sampled from the coastal exposure at Djupvik 2. The Mulde Formation occurs approximately two graptolite biozones above the Slite Formation, within the Homerian Stage of the Wenlock succession. This interval correlates with the middle part of the *Ozarkodina bohémica* Biozone, and includes a graptolite fauna typical of the *Gothograptus nassa*–*Monograptus dubius* Biozone (*sensu* Jaeger 1991), although rare evidence for the succeeding *Colonograptus? praedeubeli* Biozone has been found at other localities along strike. The clay beds were thus

deposited very close to or just above the boundary between these two zones. Jeppsson (1997a) identified the interval with the clay beds as having formed during the recovery part of the Mulde Secundo–Secundo Event.

Previous work on volcanogenic clays from Gotland (Batchelor & Jeppsson, 1994) highlighted the existence of two distinct metabentonites in the Llandovery (Lower Visby Formation). Their biostratigraphic age can now be more precisely determined than before using the newly established detailed conodont zonation for this interval (Jeppsson 1997a, 1997b; Jeppsson, unpub. data). Milankovitch cycles, identified over the interval containing these metabentonites, are about 31 000 years duration. Assuming a constant rate of sedimentation through this interval indicates that the Lusklint metabentonite was deposited *c.* 30 000 years before the end of the *Pterospathodus amorphognathoides* Biozone, and the Ireviken metabentonite *c.* 3000 years after the start of the upper *Pseudooneothodus bicornis* Biozone.

These Llandovery metabentonites, which are well exposed along the northwest coast of Gotland, could easily be correlated within the island and have the potential for more distant correlations. High-resolution correlation of Silurian sequences between Gotland and Estonia using conodonts and the Ireviken Bentonite (Jeppsson & Männik, 1993) have highlighted the correlation potential of these time markers. However, the Slite beds, which form part of the central core of the island, are well exposed only in the large Slite Quarry, and are not easily traced across the country. The only other reasonable exposure of the Slite beds, at Idå 2 (Laufeld, 1974), is considered to represent a slightly older horizon on the basis of palaeontological studies (Jeppsson, pers. comm. 1999). The Mulde Beds occupy a restricted tract of land with limited coastal exposure in the southwest of the island. Finding these highly distinctive metabentonites in deep-water graptolite successions could provide important datum planes for conflating Upper Silurian conodont and graptolite biozonations.

## 2. Mineralogy

Each clay sample was disaggregated ultrasonically and the < 2 µm fraction was sedimented onto a glass slide by pipette to produce an orientated sample. This clay fraction was subjected to XRD analysis, in both the dried state and after glycolation. The interpretation of the x-ray diffractograms followed the method described by Srodon (1980). A split of the sample was disaggregated using sodium hexametaphosphate, washed free of clay, and sieved to < 500 µm. The residue was dried, and separated into light and heavy fractions using tetrabromoethane (specific gravity: 2.9). Table 1 lists the major clay and heavy-mineral components identified.

The existence of identifiable illite/smectite mixed

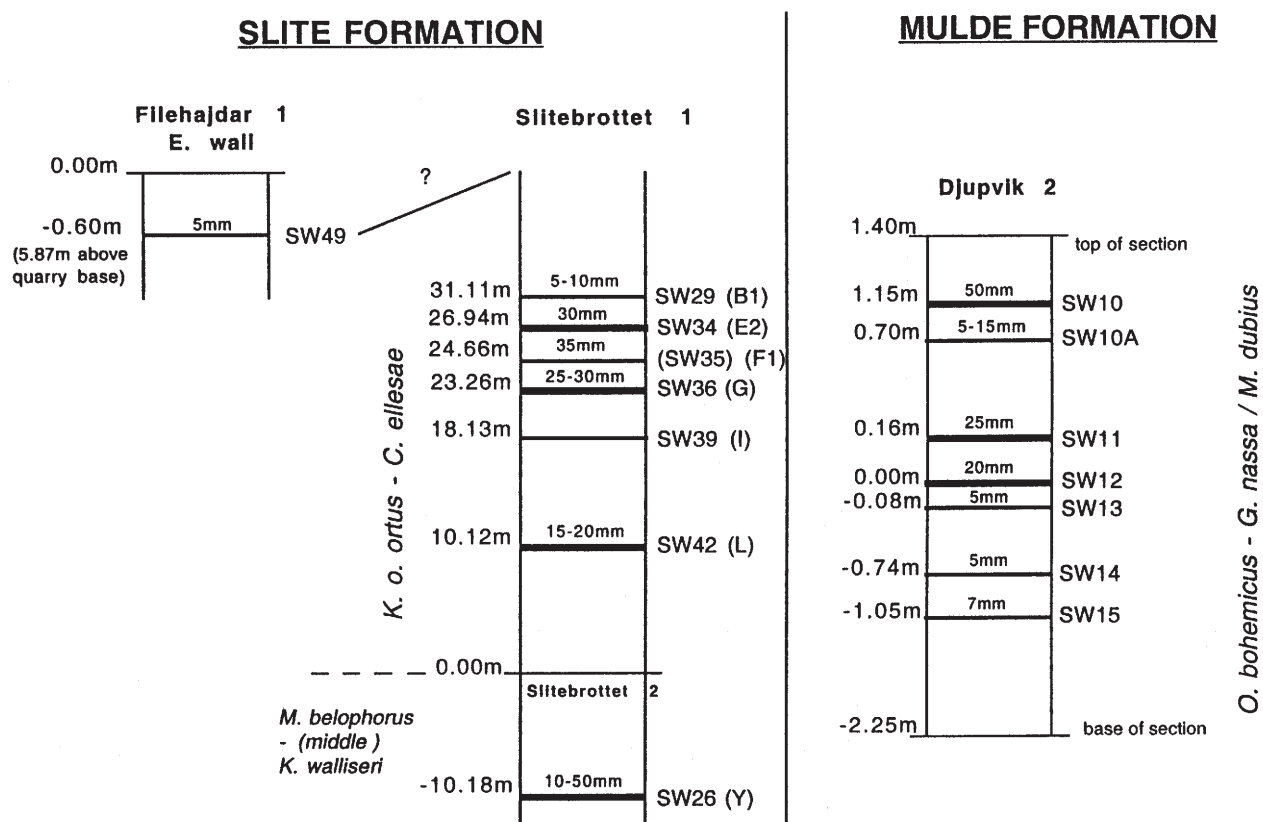


Figure 2. Schematic log sections of the sampling localities, showing the thickness and distribution of metabentonite beds. The letter after the SW sample numbers refers to a local classification scheme. Biozones are indicated by both conodont and graptolite species.

layer clays and the presence of euhedral crystals of apatite, biotite and occasionally zircon (Fig. 3), suggests that these clays are volcanogenic, or at least have a volcanogenic component (Ross & Shannon, 1926). The preponderance of illite to smectite in all but one sample allows these clays to be defined as metabentonites (Gary, McAfee & Wolf, 1977).

### 3. Geochemistry

Samples from the Slite and Mulde Formations were analyzed for their major and trace element components by XRF using standard fused-bead and pressed-powder-pellet techniques with a Philips PW1450/20 XRF with a wavelength-dispersive detector, calibrated using an internal reference sample and international geochemical standards (Table 2). In addition, euhedral microphenocrysts of apatite, between 20 and 200  $\mu\text{m}$  long, were extracted, dissolved in nitric acid and analyzed for their REE and selected trace-element content using inductively-coupled plasma-mass spectrometry (ICP-MS). Indium was used as the internal calibrating standard (Table 3).

#### 3.a. Whole-rock geochemistry

In order to assess the relative contribution of detrital clay to the volcanoclastic component, shale-normalized plots are used, based on the method of Wray

(1995). Selected elements were normalized to the USGS geochemical reference sample SCo-1 (Cody Shale) (Govindaraju, 1994) and are shown in Figure 4. In general, the Slite suite shows greater deviation from 1 particularly for Th, Nb and Zr. The low values for sample SW49 are due to a large proportion of CaO, which dilutes the absolute abundance of all other elements. The Mulde suite shows a more attenuated distribution, although Th, Nb and Zr are generally

Table 1. Clay and heavy-mineral composition of Slite and Mulde metabentonites

| Sample number | Local designation | I/Sm % | Other clays | Heavy minerals  |
|---------------|-------------------|--------|-------------|-----------------|
| Slite         |                   |        |             |                 |
| SW49          |                   | 100    | Chl         | Ap, Bi, Zir     |
| SW29          | B1                | 78     | Chl         | Ap, Bi, Py      |
| SW34          | E2                | 81     |             | Ap, Bi, Py      |
| SW36          | G                 | 58     | Chl         | Ap, Bi, Py      |
| SW39          | I                 | n.d.   | Chl, Kaol   | Ap, Bi, Py      |
| SW42          | L                 | 90     | Chl         | Ap, Bi, Py, Zir |
| SW26          | Y                 | 85     | Kaol        | Ap, Bi, Py      |
| Mulde         |                   |        |             |                 |
| SW10          | +1.15m            | 70     | Chl         | Ap, Bi, Py      |
| SW10A         | +0.70m            | n.d.   | Chl         | Ap, Bi, Py, Jar |
| SW11          | +0.16m            | 65     | Chl         | Ap, Bi, Py, Zir |
| SW12          | 0.00m             | 46     | Chl         | Ap, Bi, Py, Zir |
| SW14          | -0.74m            | 85     | Chl         | Ap, Bi, Py      |

I/Sm% (illite/smectite) calculated using the method of Srodon (1980). Abbreviations: Chl, Chlorite; Kaol, Kaolinite; Ap, Apatite; Bi, Biotite; Py, Pyrite; Zir, Zircon; Jar, Jarosite; and n.d., not determined

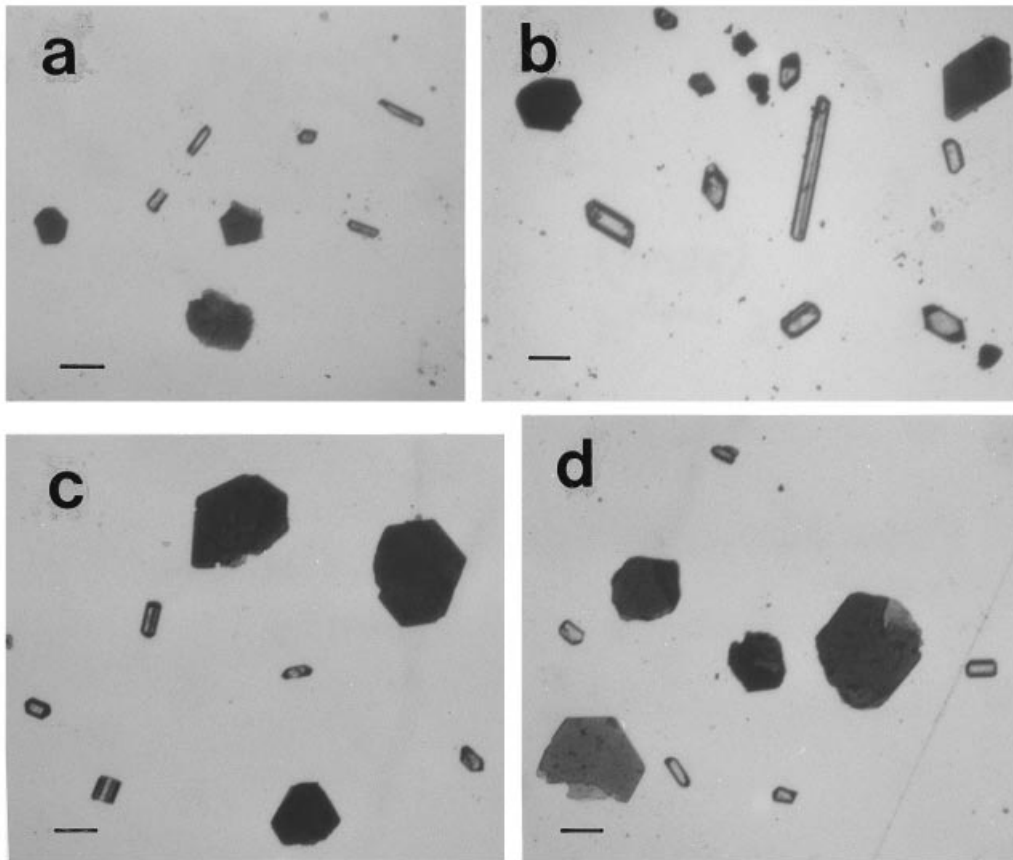


Figure 3. Photographs showing the morphology of microcrystals. Scale bar: 20  $\mu\text{m}$ . (a) SW29: biotite and apatite (Slite). (b) SW42: biotite, apatite, zircon (Slite). (c) SW11: biotite, apatite, zircon (Mulde). (d) SW14: biotite, apatite (Mulde).

higher. These three elements can be attributed to the presence of biotite, apatite and, in some samples, zircon of volcanic origin. For comparison, a mudstone from Gotland is superimposed (SW79, a 20 mm-thick clay 1.79 m above the beach level at Ygne; Lower Visby 'e' horizon) which emphasizes the lack of a volcanoclastic component.

These clays were deposited in a shallow carbonate platform environment (Laufeld & Bassett, 1981), and it is inevitable that rapid precipitation of carbonate occurred and some reworking of the volcanic ash took place. Calcium carbonate and pyrite are common constituents of most Gotland clays, and this effect is seen in the relatively high CaO, MgO,  $\text{Fe}_2\text{O}_3$  and LOI values (Table 2). In view of this carbonate contamination, discussion of whole-rock geochemical data is restricted to six elements that are traditionally considered to be the least mobile during diagenesis: Ti, Th, Zr, Nb, Ce and Y. Since conodonts from Gotland show no colour change, and hence no detectable thermal effects (Odin *et al.* 1984), it can confidently be assumed that these trace elements were not mobilized by post-diagenetic processes. They are utilized as three ratios plotted on a triangular diagram (Fig. 5). All samples plot between the calc-alkaline dacite and rhyolite fields, except two Mulde samples (SW10 and SW14), which trend towards alkaline compositions.

### 3.b. Apatite geochemistry

The chondrite-normalized REE diagrams (Fig. 6) show general LREE-enrichment patterns for all the samples. The absence of a positive Ce anomaly, which might be expected in a reducing sedimentary environment that has generated pyrite, excludes a diagenetic origin for the apatite (Wright, Scrader & Holser, 1987). It is therefore assumed that the euhedral apatite microphenocrysts in these metabentonites are of magmatic origin, and the distribution of REE in the apatites reflects the composition of their host magma (Fleet & Pan, 1997).

However, superimposed upon the general REE pattern, a difference in the magnitude of the negative Eu\* anomaly ( $-\text{Eu}^*$ ), ( $-\text{Eu}^* = \text{Eu}_n / ((\text{Sm}_n + \text{Gd}_n) / 2)$ ), exists between samples in the Slite and Mulde assemblages. The former generally have a less-pronounced anomaly suggesting a lower degree of feldspar fractionation in the parental magma with the exception of samples SW42 (L horizon) and SW49, both of which show pronounced  $-\text{Eu}^*$ , similar to the Mulde suite. The latter sample (SW49) is the youngest of the Slite suite, collected from Filehajdar 1 quarry, and may be a precursor of the volcanism that generated the Mulde suite. This depletion in Eu is consistent with increased plagioclase feldspar fractionation, suggesting that the



Table 2. Whole-rock geochemical data for Slite and Mulde metabentonites

| Local designation<br>Sample    | Slite metabentonites |           |           |           |            |            |       | Mulde metabentonites |                 |               |               |                |                       | Cody<br>Shale<br>SCo-1 |
|--------------------------------|----------------------|-----------|-----------|-----------|------------|------------|-------|----------------------|-----------------|---------------|---------------|----------------|-----------------------|------------------------|
|                                | Y<br>SW26            | L<br>SW42 | I<br>SW39 | G<br>SW36 | E2<br>SW34 | B1<br>SW29 | SW49  | +1.15m<br>SW10       | +0.70m<br>SW10A | +0.16<br>SW11 | 0.00m<br>SW12 | -0.74m<br>SW14 | Error<br>$\pm 2$ S.D. |                        |
| Oxide %                        |                      |           |           |           |            |            |       |                      |                 |               |               |                |                       |                        |
| SiO <sub>2</sub>               | 46.87                | 39.74     | 44.63     | 39.17     | 47.41      | 42.10      | 15.51 | 48.85                | 40.3            | 51.08         | 47.99         | 44.66          | 0.4                   | 62.78                  |
| TiO <sub>2</sub>               | 0.91                 | 0.55      | 0.83      | 0.59      | 0.71       | 0.59       | 0.28  | 0.53                 | 0.54            | 0.68          | 0.66          | 0.68           | 0.08                  | 0.628                  |
| Al <sub>2</sub> O <sub>3</sub> | 20.94                | 13.48     | 15.38     | 11.23     | 16.17      | 10.79      | 5.48  | 15.22                | 10.77           | 14.85         | 14.17         | 13.58          | 0.15                  | 13.67                  |
| Fe <sub>2</sub> O <sub>3</sub> | 6.56                 | 3.86      | 6.10      | 4.76      | 5.72       | 4.17       | 2.57  | 4.15                 | 4.61            | 5.64          | 5.69          | 5.64           | 0.1                   | 5.14                   |
| MnO                            | 0.04                 | 0.03      | 0.04      | 0.05      | 0.04       | 0.04       | 0.03  | 0.04                 | 0.04            | 0.03          | 0.04          | 0.04           | 0.01                  | 0.052                  |
| MgO                            | 2.64                 | 4.16      | 4.56      | 5.47      | 4.64       | 4.49       | 2.34  | 3.84                 | 4.46            | 4.21          | 4.12          | 4.27           | 0.1                   | 2.72                   |
| CaO                            | 3.77                 | 14.87     | 7.08      | 14.26     | 5.97       | 14.58      | 38.90 | 7.2                  | 16.05           | 5.85          | 8.26          | 10.56          | 0.05                  | 2.62                   |
| Na <sub>2</sub> O              | 0.30                 | 0.67      | 0.24      | 0.27      | 0.70       | 0.81       | 1.00  | 0.33                 | 0.73            | 0.78          | 0.77          | 0.71           | 0.2                   | 0.9                    |
| K <sub>2</sub> O               | 4.44                 | 4.14      | 5.31      | 4.02      | 5.36       | 3.47       | 1.72  | 4.64                 | 3.4             | 4.94          | 4.57          | 4.33           | 0.08                  | 2.77                   |
| P <sub>2</sub> O <sub>5</sub>  | 0.08                 | 0.07      | 0.13      | 0.08      | 0.09       | 0.02       | 0.03  | 0.05                 | 0.08            | 0.07          | 0.07          | 0.09           | 0.05                  | 0.206                  |
| LOI                            | 9.00                 | 17.40     | 11.60     | 16.80     | 11.00      | 17.40      | 32.00 | 13.2                 | 17.4            | 10.4          | 12.2          | 13.4           |                       | [8.8]                  |
| Element ppm                    |                      |           |           |           |            |            |       |                      |                 |               |               |                |                       |                        |
| Nb                             | 26                   | 22        | 14        | 12        | 16         | 10         | 4     | 17                   | 10              | 16            | 18            | 13             | 5                     | 11                     |
| Zr                             | 412                  | 292       | 253       | 223       | 229        | 198        | 74    | 153                  | 155             | 268           | 284           | 175            | 25                    | 160                    |
| Y                              | 31                   | 19        | 24        | 19        | 23         | 19         | 10    | 16                   | 22              | 24            | 27            | 19             | 5                     | 26                     |
| Sr                             | 150                  | 143       | 107       | 129       | 97         | 116        | 146   | 125                  | 268             | 134           | 152           | 194            | 3                     | 174                    |
| Rb                             | 105                  | 105       | 93        | 91        | 127        | 104        | 58    | 132                  | 110             | 137           | 130           | 130            | 3                     | 112                    |
| Th                             | 30                   | 27        | 15        | 13        | 16         | 12         | 6     | 15                   | 13              | 20            | 23            | 14             | 5                     | 9.7                    |
| Pb                             | 81                   | 27        | 42        | 40        | 29         | 23         | 24    | 27                   | 15              | 30            | 34            | 21             | 5                     | 31                     |
| Ga                             | 16                   | 17        | 17        | 16        | 20         | 17         | 15    | 20                   | 17              | 18            | 20            | 21             | 3                     | 15                     |
| Zn                             | 43                   | 44        | 44        | 42        | 53         | 46         | 50    | 44                   | 47              | 56            | 55            | 56             | 5                     | 103                    |
| Ni                             | 20                   | 23        | 25        | 23        | 31         | 28         | 21    | 34                   | 35              | 40            | 41            | 42             | 10                    | 27                     |
| Ce                             | 59                   | 59        | 57        | 61        | 60         | 43         | 30    | 50                   | 57              | 69            | 63            | 66             | 20                    | 62                     |
| Sc                             | 3                    | 18        | 11        | 15        | 11         | 19         | 50    | 14                   | 19              | 11            | 13            | 14             | 5                     | 10.8                   |
| V                              | 83                   | 58        | 73        | 61        | 106        | 75         | 69    | 63                   | 73              | 78            | 79            | 84             | 15                    | 131                    |
| Ba                             | 271                  | 337       | 269       | 250       | 321        | 354        | 227   | 333                  | 477             | 375           | 384           | 383            | 50                    | 570                    |
| La                             | 13                   | 22        | 16        | 29        | 28         | 27         | 17    | 24                   | 31              | 24            | 29            | 27             | 10                    | 29.5                   |

Mulde suite is generally more evolved than Slite. The Mulde samples show a trimodal compositional spectrum, with SW10 (at +1.15 m) showing the least evolved character, SW11 (at +0.16 m) and SW12 (at 0.00 m, reference level) having a REE-enriched signature and SW10A (at +0.70 m) and SW14 (at -0.74 m) sharing a steep chondrite-normalized REE curve, indicative of evolved or alkaline magmas. This fluctuation in chemical composition through time could indicate separate magmatic sources, or an origin from a compositionally zoned magma source.

The Ce/Y value of apatite has been used to define the alkalinity of the host melt (Roeder *et al.* 1987), with values above 7.7 considered to represent highly alkaline environments. On this basis, samples SW10A and SW14, with the highest Ce/Y values (9.2 and 7.6 respectively), have alkaline affinities, and support the existence of an independent magma source for these Mulde samples.

Figure 7 uses two important REE parameters: -Eu\*, indicative of the degree of plagioclase feldspar fractionation, and Ce<sub>n</sub>/Yb<sub>n</sub>, which reflects the relative enrichment of LREE or depletion of HREE in the parental melt. Higher values (Ce<sub>n</sub>/Yb<sub>n</sub> ~40) could reflect the effect of crustal contamination or of low-degree partial melting from a mantle source. According to Watson & Green (1981), the apatite structure does not normally concentrate LREE relative to HREE. However Roeder *et al.* (1987) reported

that many apatites show a LREE enrichment and that this feature reflects crystallization from a LREE-enriched magma. This observation of LREE enrichment in apatites has been explained by Hughes, Cameron & Mariano, (1991), who investigated the bond-valence sums for all REE in four natural apatites. Their study showed that the Ca(2) site is favoured by the elements La to Sm, with Nd having the highest partition coefficient. Therefore, the chondrite-normalized REE pattern should show a concave-downward distribution, with LREE > HREE. This feature is seen in all the Wenlock apatites in this study.

Two Slite samples (SW42 and SW49) fall into the low -Eu\* category, which in turn represents more evolved compositions. For comparison, data for apatite taken from Telychian metabentonites from Norway (Batchelor, Weir & Spjeldnaes, 1995), are superimposed. The appellation of these Norwegian metabentonites as 'evolved' or 'primitive' was based on the relative concentrations of high field strength elements (HFSE) (Zr, Nb, Th), Ni and Ti. These two Slite samples plot close to the 'evolved' Norwegian suite and the Ireviken metabentonite (IB) from Gotland (Batchelor & Jeppsson, 1994). The rest of the Slite suite plot with the 'primitive' Norwegian suite and the Lusklint metabentonite (LB) from Gotland.

In contrast, the younger Mulde suite shows a range of values, from highly fractionated 'evolved' environments (SW11, SW12) to the alkaline, LREE-

Table 3. REE and selected trace element data for apatite microphenocrysts in Slite and Mulde metabentonites

| Local designation    | Y      |                | L      |                | I      |                | G     |               | E2     |                |           |                |
|----------------------|--------|----------------|--------|----------------|--------|----------------|-------|---------------|--------|----------------|-----------|----------------|
| Sample               | SW26   | error<br>±1 SD | SW42   | error<br>±1 SD | SW39   | error<br>±1 SD | SW36  | error<br>±1SD | SW34   | error<br>±1 SD | SW49      | error<br>±1 SD |
| ppm                  |        |                |        |                |        |                |       |               |        |                |           |                |
| La                   | 1625   | 55             | 1258   | 16             | 724    | 22             | 500   | 8             | 736    | 7              | 639       | 6              |
| Ce                   | 4044   | 86             | 3277   | 82             | 1889   | 44             | 1232  | 6             | 1771   | 29             | 1582      | 45             |
| Pr                   | 550    | 15             | 443    | 8              | 266    | 12             | 164   | 1             | 224    | 2              | 189       | 6              |
| Nd                   | 2349   | 47             | 1846   | 61             | 1174   | 36             | 686   | 35            | 963    | 47             | 708       | 56             |
| Sm                   | 442    | 18             | 331    | 12             | 219    | 6              | 131   | 10            | 162    | 12             | 113       | 20             |
| Eu                   | 97.8   | 2.5            | 40.6   | 2.1            | 52.6   | 1.7            | 28    | 1.7           | 40.3   | 5.3            | 16.4      | 3.7            |
| Gd                   | 371    | 10             | 302    | 7              | 195    | 9              | 105   | 7             | 145    | 8              | 122       | 11             |
| Tb                   | 36.5   | 0.4            | 33.6   | 0.3            | 18.7   | 0.9            | 9.8   | 0.5           | 15.8   | 5.5            | 12.3      | 1.7            |
| Dy                   | 171    | 7              | 181    | 7              | 92.2   | 4              | 55    | 4.8           | 68.9   | 8.1            | 87        | 18.4           |
| Ho                   | 21.4   | 0.8            | 28.2   | 0.7            | 11.7   | 0.9            | 6.7   | 1             | 12     | 6.1            | 14.6      | 1.6            |
| Er                   | 49.4   | 4.9            | 73.1   | 4.3            | 26.9   | 3.4            | 14.3  | 1.8           | 19.8   | 8.4            | 36.4      | 5.9            |
| Tm                   | 4.2    | 1              | 7.8    | 0.2            | 2.8    | 0.5            | 1.2   | 0.3           | 3.8    | 3.9            | 3.8       | 2.1            |
| Yb                   | 22.7   | 4.2            | 41.3   | 2.6            | 14.2   | 3.5            | 7.1   | 1.7           | 7.3    | 2.9            | 24.6      | 9.6            |
| Lu                   | 2      | 1              | 5.9    | 1              | 1.5    | 0.5            | 0.4   | 0.1           | 2.1    | 2.1            | 1         | 1.4            |
| ΣREE                 | 9786   |                | 7868   |                | 4688   |                | 2941  |               | 4171   |                | 3549      |                |
| Mn                   | 563    | 15             | 953    | 12             | 605    | 19             | 345   | 26            | 376    | 13             | 1025      | 46             |
| Sr                   | 4045   | 80             | 531    | 12             | 4356   | 79             | 1851  | 21            | 3048   | 59             | 424       | 13             |
| Y                    | 583    | 14             | 743    | 7              | 331    | 10             | 197   | 2             | 251    | 8              | 425       | 19             |
| Th                   | 356    | 13             | 431    | 3              | 186    | 7              | 96.7  | 6             | 216    | 6              | 72.8      | 8              |
| U                    | 16.3   | 2.7            | 16.1   | 1.4            | 7.5    | 0.7            | 5.7   | 1             | 10.3   | 5              | 14.8      | 2.7            |
| Ce/Yb                | 178.1  |                | 79.3   |                | 133    |                | 173.5 |               | 242.6  |                | 64.3      |                |
| Eu/Eu*               | 0.72   |                | 0.39   |                | 0.76   |                | 0.71  |               | 0.79   |                | 0.42      |                |
| (Ce/Yb) <sub>n</sub> | 46.3   |                | 20.5   |                | 34.4   |                | 44.9  |               | 63.1   |                | 16.6      |                |
| Ce/Y                 | 6.9    |                | 4.4    |                | 5.7    |                | 6.2   |               | 7      |                | 3.7       |                |
| Local designation    | +1.15m |                | +0.70m |                | +0.16m |                | 0.00m |               | -0.74m |                |           |                |
| Sample               | SW10   | error<br>±1 SD | SW10A  | error<br>±1 SD | SW11   | error<br>±1 SD | SW12  | error<br>±1SD | SW14   | error<br>±1 SD | Chondrite |                |
| ppm                  |        |                |        |                |        |                |       |               |        |                |           |                |
| La                   | 500    | 24             | 1248   | 2              | 1611   | 18             | 1396  | 17            | 1183   | 21             | 0.2446    |                |
| Ce                   | 1362   | 5              | 2818   | 30             | 4266   | 46             | 3771  | 92            | 2810   | 8              | 0.6379    |                |
| Pr                   | 197    | 15             | 321    | 3              | 583    | 3              | 506   | 18            | 333    | 4              | 0.09637   |                |
| Nd                   | 906    | 69             | 1171   | 42             | 2560   | 89             | 2209  | 30            | 1312   | 60             | 0.4738    |                |
| Sm                   | 182    | 25             | 170    | 18             | 493    | 30             | 422   | 39            | 200    | 10             | 0.154     |                |
| Eu                   | 30.1   | 5.7            | 25.8   | 2.2            | 36.8   | 5.4            | 37.1  | 1.6           | 29.5   | 1.8            | 0.05802   |                |
| Gd                   | 234    | 13             | 153    | 6              | 480    | 25             | 402   | 24            | 181    | 11             | 0.2043    |                |
| Tb                   | 30.6   | 3.8            | 16.4   | 0.7            | 54.9   | 2.4            | 50.5  | 2.4           | 17.8   | 1.5            | 0.03745   |                |
| Dy                   | 205    | 23             | 78.1   | 5.2            | 301    | 20             | 254   | 21            | 98.6   | 6.5            | 0.2541    |                |
| Ho                   | 32.9   | 5.2            | 11.1   | 1.7            | 46.6   | 0.4            | 38.8  | 0.4           | 15.1   | 3.1            | 0.0567    |                |
| Er                   | 84.1   | 16.2           | 27.3   | 2.1            | 114    | 12             | 97.7  | 7.5           | 36.5   | 4.2            | 0.166     |                |
| Tm                   | 5.4    | 0.6            | 2.2    | 1              | 11.4   | 1.5            | 8.4   | 1.1           | 3.9    | 0.6            | 0.02561   |                |
| Yb                   | 39     | 11.4           | 16.5   | 2.7            | 60.3   | 6.5            | 50.1  | 11.8          | 21.1   | 3.6            | 0.1651    |                |
| Lu                   | 1.6    | 0.7            | 2.2    | 0.7            | 7.5    | 0.7            | 6.1   | 1.9           | 2.1    | 0.6            | 0.02539   |                |
| ΣREE                 | 3810   |                | 6061   |                | 10625  |                | 9249  |               | 6244   |                |           |                |
| Mn                   | 2064   | 81             | 814    | 14             | 704    | 23             | 695   | 26            | 951    | 22             |           |                |
| Sr                   | 612    | 38             | 720    | 17             | 495    | 8              | 563   | 25            | 861    | 1              |           |                |
| Y                    | 864    | 12             | 306    | 6              | 1203   | 13             | 1005  | 30            | 368    | 4              |           |                |
| Th                   | 72     | 10             | 67     | 3              | 92     | 3              | 83    | 6             | 80     | 3              |           |                |
| U                    | 8.1    | 1.4            | 14.2   | 0.5            | 12.9   | 2              | 13.9  | 2.3           | 17.4   | 2.8            |           |                |
| Ce/Yb                | 35     |                | 171    |                | 71     |                | 75    |               | 133    |                |           |                |
| Eu/Eu*               | 0.45   |                | 0.48   |                | 0.23   |                | 0.27  |               | 0.47   |                |           |                |
| (Ce/Yb) <sub>n</sub> | 9      |                | 44.2   |                | 18.3   |                | 19.5  |               | 34.4   |                |           |                |
| Ce/Y                 | 1.6    |                | 9.2    |                | 3.5    |                | 3.8   |               | 7.6    |                |           |                |

enriched/HREE-depleted apatite (SW10A, SW14). Coincidentally, samples SW11 and SW12 both contain zircon as an accessory phase, whereas the alkaline SW10A and SW14 do not. This is consistent with the instability of zircon in alkaline melts (Watson 1979).

The consensus of the chemical compositions suggests three broad associations: Slite samples with high (Ce/Yb)<sub>n</sub> and low -Eu\*, two Mulde samples with alkaline characteristics, and a loose grouping with low Ce<sub>n</sub>/Yb<sub>n</sub> and high -Eu\*.

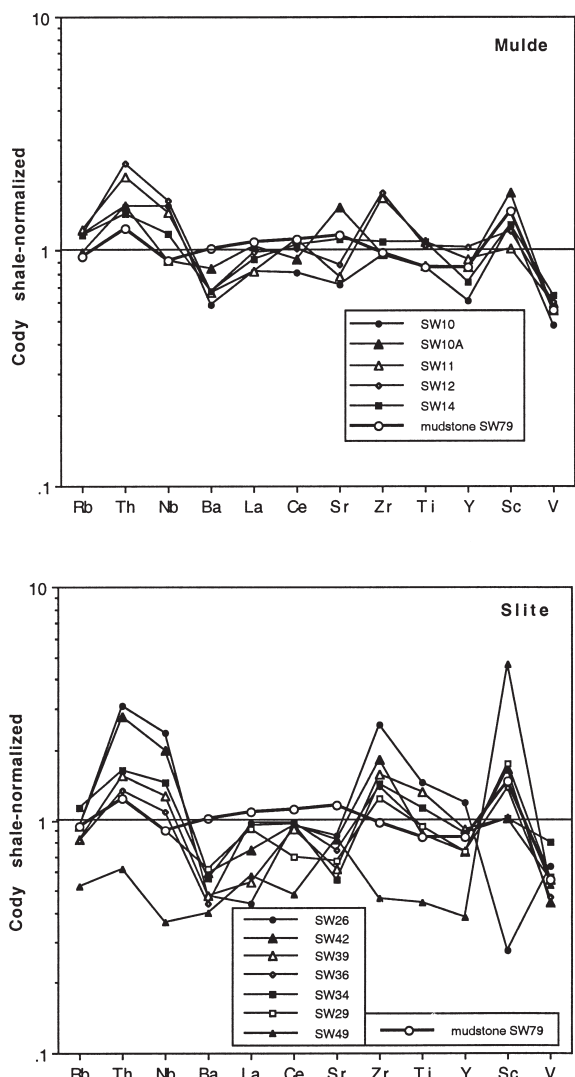


Figure 4. Cody shale-normalized plots for selected elements from the Slite and Mulde metabentonites.

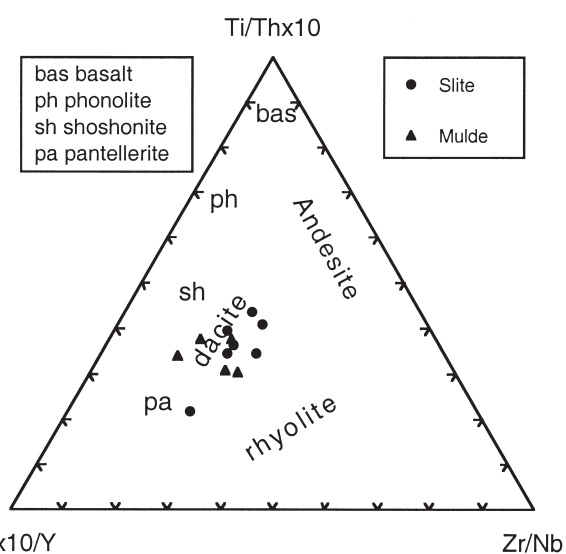


Figure 5. Triangular diagram showing the distribution of Wenlock metabentonites based on  $Ti/Thx_{10}$ ,  $Cex_{10}/Y$  and  $Zr/Nb$  data. Volcanic-rock fields are based on data from Wilson (1989).

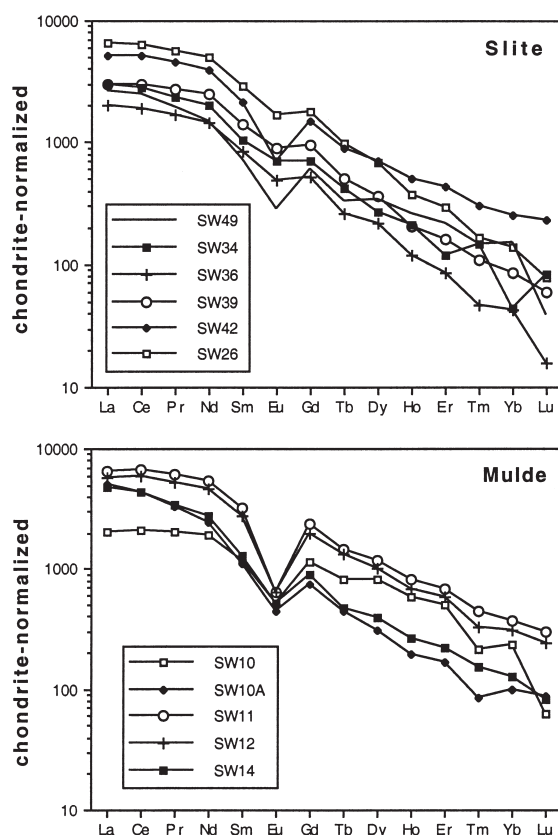


Figure 6. Chondrite-normalized REE graphs for Slite and Mulde apatites. Normalizing values from Evensen, Hamilton & O'Nions (1978). Data for Pm, between Nd and Sm, are not available.

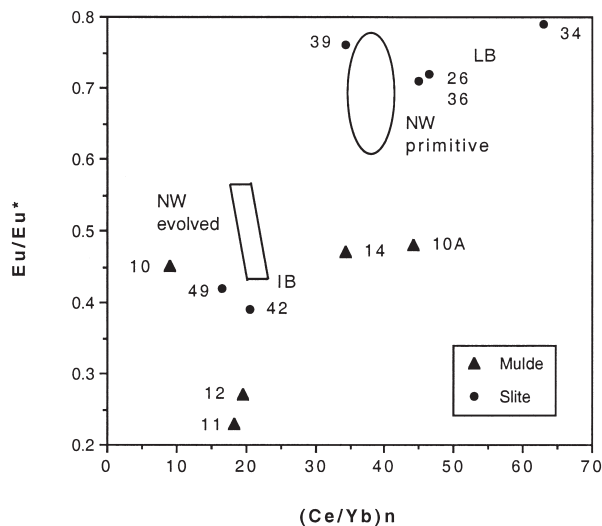


Figure 7. Bivariate plot of  $(Ce/Yb)_n - Eu/Eu^*$  for Wenlock apatite microphenocrysts. Fields for both 'evolved' and 'primitive' Norwegian apatite samples (NW) are superimposed (data from Batchelor, Weir & Spjeldnaes, 1995). Two apatite samples from Llandovery metabentonites from Gotland are also included. Abbreviations: IB, Ireviken metabentonite; LB, Lusklint metabentonite (data from Batchelor & Jeppsson, 1994).



#### 4. Source and tectonic setting

Contemporaneous coarse-grained ashes of *C. lundgreni* Biozone age found in Bornholm were postulated to have been derived some 300 km to the south (Bjerreskov & Jørgensen, 1983), implying the existence of active volcanism in Upper Wenlock times to the south of Gotland.

The closest known site to Gotland of Silurian (Ludlovian) volcanism is along the closing Tornquist Suture Zone at Klodsko in Poland (Oliver, Corfu & Krogh, 1993) about 800 km south-southwest of Gotland. Silurian volcanism has also been described in the Brabant Massif of Belgium, where calc-alkaline volcanism is believed to have ended in the Wenlock with an acidic ash fall (André, Hertogen & Deutsch, 1986). Extrusive silicic volcanism is also recorded in late Llandovery–early Wenlock times in the Neuville-sous-Huy area of Belgium (Verniers & Van Grootel, 1991). However, being of *c.* 1150 km to the southwest, these Belgian sources may be unlikely candidates for providing the Gotland ash falls.

The Tornquist–Teyseyre Zone (TTZ), the northernmost expression of the Trans-European Suture Zone, lies 400 km southwest of Gotland, while the Elbe Line, which is now believed to mark the southwest margin of Baltica, is 250 km southwest of Bornholm and 650 km to the southwest of Gotland (Cocks, McKerrow & van Stall, 1997). Potential volcanic sources in Norway are discounted, because the bulk of Caledonian igneous activity appears to have ended towards the top of the Llandovery (Pedersen, Furnes & Dunning, 1991). However, Wenlock metabentonites are known from the Steinsfjord Formation, near Oslo (Nils Spjeldnaes, pers. comm. 1990).

The chemical composition of the upper Llandovery Luskint metabentonite from Gotland, characterized by high  $\Sigma$ REE content in apatite (>1%), LREE > HREE and the absence of zircon microphenocrysts, suggested that alkaline magma may have been responsible for its formation (Batchelor & Jeppsson, 1994).

The Wenlock epoch is regarded as the time when the Iapetus and Tornquist oceans closed (Williams, O'Connor & Menuge, 1992; Trench & Torsvik, 1992; Soper *et al.* 1992). A waning subduction zone, with thickening crust, can give rise to alkaline magmas rich in HFSE and with potassic affinities, such as are found today in the form of shoshonite lavas at Stromboli, Aeolian Islands, which lies above 18 km of continental crust (Francalanci, Manetti & Peccerillo, 1989). Ascending melts interact extensively with the thick crust, generating magmas enriched in lithophile elements, such as the LREE. This scenario could have given rise to the two alkaline Mulde metabentonites SW10A and SW14. It is also possible to generate K-rich melts through fractional crystallization of high-alumina tholeiitic basalt at ~10 kbar (*c.* 30 km depth). Crystallization of plagioclase feldspar, hypers-

thene and augite generates a K-rich melt with little or no change in SiO<sub>2</sub> (Meen, 1987). This process would also concentrate the LREE into the melt. Apatite crystallizing in such an environment would inherit a –Eu\* and an enriched LREE profile, as seen in this study.

#### 5. Conclusion

In summary, the Wenlock metabentonites were generated by ash falls from evolved silicic and alkaline explosive volcanism. The most likely location for the source volcanoes was along the Tornquist–Teyseyre Zone some 400 km southwest of Gotland. Such a source could provide ash, which would fan out northwards in a plume wide enough to reach Bornholm, the Oslo region and Gotland. Bornholm, being some 100 km northeast of the Tornquist–Teyseyre Zone, would receive coarser material.

It is suggested that the Slite and Mulde metabentonites were deposited by ash falls from three separate volcanic sources, each of which erupted randomly throughout this period of time, so it is not possible to associate a stratigraphical unit with a specific type of volcanism. Nevertheless, the value of these data lies in the fact that adjacent metabentonites have contrasting apatite compositions that can be correlated with metabentonite sequences elsewhere. While these metabentonites could not be unequivocally correlated within the island of Gotland due to poor exposure, their chemically distinct nature makes them suitable candidates for correlation work in Wenlock successions in other regions of northern Europe.

**Acknowledgements.** Fieldwork on Gotland, based at the Allekvia Geological Field Station, Endre, was funded by the Carnegie Trust and analytical work was funded by a Leverhulme Trust grant to R. A. B. L. J. is funded by the Swedish Natural Science Research Council. Thanks are extended to Richard Hinton, Jeremy Preston and an anonymous reviewer for comments made on an earlier draft of this paper. Warren Huff and David Wray improved this version.

#### References

- ANDRÉ, L., HERTOGEN, J. & DEUTSCH, S. 1986. Ordovician–Silurian magmatic provinces in Belgium and the Caledonian orogeny in middle Europe. *Geology* **14**, 879–82.
- BATCHELOR, R. A. & JEPSSON, L. 1994. Late Llandovery bentonites from Gotland, Sweden, as chemostratigraphic markers. *Journal of the Geological Society, London* **151**, 741–6.
- BATCHELOR R. A., WEIR, J. A. & SPJELDNAES, N. 1995. Geochemistry of Telychian metabentonites from Vik, Ringerike District, Oslo Region. *Norsk Geologisk Tidsskrift* **75**, 219–28.
- BJERRESKOV, M. & JØRGENSEN, K. Å. 1983. Late Wenlock graptolite-bearing tuffaceous sandstone from Bornholm, Denmark. *Bulletin of the Geological Society of Denmark* **31**, 129–49.
- COCKS, L. R. M., MCKERROW, W. S. & VAN STALL, C. R. 1997. The margins of Avalonia. *Geological Magazine* **134**, 627–36.

- EVENSEN, N. M., HAMILTON, P. J. & O'NIONS, R. K. 1978. Rare-earth abundances in chondrite meteorites. *Geochimica et Cosmochimica Acta* **42**, 1199–212.
- FLEET, M. E. & PAN, Y. 1997. Site preferences of rare-earth elements in fluorapatite: binary (LREE + HREE) substituted crystals. *American Mineralogist* **82**, 870–7.
- FORTEY, N. J., MERRIMAN, R. J. & HUFF, W. D. 1996. Silurian and late-Ordovician K-bentonites as a record of late Caledonian volcanism in the British Isles. *Transactions of the Royal Society of Edinburgh: Earth Sciences* **86**, 167–80.
- FRANCALANCI, L., MANETTI, P. & PECCERILLO, A. 1989. Volcanological and magmatological evolution of Stromboli volcano (Aeolian Islands): the role of fractional crystallisation, magma mixing, crustal contamination and source heterogeneity. *Bulletin Volcanologique* **51**, 355–78.
- GARY, M., MCAFEE, R. JR & WOLF, C. L. (eds) 1977. *Glossary of Geology*. Washington: American Geological Institute, 806 pp.
- GOVINDARAJU, K. 1994. Compilation of working values and sample descriptions from 383 geostandards. *Geostandards Newsletter* **18**, Special Issue, p. 16.
- HEDE, J. E. 1960. The Silurian of Gotland. In *The Lower Palaeozoic of Scania*. (eds G. Regnell and J. E. Hede). Nodren, Sweden: International Geological Congress XXI Session.
- HUGHES, J. M., CAMERON, M. & MARIANO, A. N. 1991. Rare-earth element ordering and structural variations in natural rare-earth-bearing apatites. *American Mineralogist* **76**, 1165–73.
- JAEGER, H. 1991. Neue Standard-Graptolithenzonenfolge nach der 'Grossen Krise' an der Wenlock/Ludlow-Grenze (Silur). *Neues Jahrbuch für Geologie und Paläontologie Abhandlung* **182**, 303–54.
- JEPPSSON, L. 1997a. Recognition of a probable secundo-primo event in the Early Silurian. *Lethaia* **29**, 311–15.
- JEPPSSON, L. 1997b. A new Latest Telychian, Sheinwoodian and Earliest Homerian (Early Silurian) standard conodont zonation. *Transactions of the Royal Society of Edinburgh. Earth Sciences* **88**, 91–114.
- JEPPSSON, L., ALDRIDGE, R. J. & DORNING, K. J. 1995. Wenlock (Silurian) oceanic episodes and events. *Journal of the Geological Society, London* **152**, 487–98.
- JEPPSSON, L. & MÄNNIK, P. 1993. High-resolution correlations between Gotland and Estonia near the base of the Wenlock. *Terra Nova* **5**, 348–58.
- LAUFELD, S. 1974. Reference localities for palaeontology and geology in the Silurian of Gotland. *Sveriges Geologiska Undersökning* **C705**, 1–172.
- LAUFELD, S. & BASSETT, M. G. 1981. Gotland: the anatomy of a Silurian carbonate platform. *Episodes* **1981**, 23–7.
- LAUFELD, S. & JEPPSSON, L. 1976. Silicification and bentonites in the Silurian of Gotland. *Geologiska Föreningens i Stockholm Förhandlingar* **98**, 31–44.
- MEEN, J. K. 1987. Formation of shoshonites from calc-alkaline basalt magmas: geochemical and experimental constraints from the type locality. *Contributions to Mineralogy and Petrology* **97**, 333–51.
- ODIN, G. S., SPIELDNAES, N., JEPPSSON, L. & NIELSEN, A. T. 1984. Field meeting in Scandinavia: possibilities of time-scale calibration of the Silurian in diverse geological (P, T) environments in Scandinavia. *Bulletin of Liasons and Informations, IGCP Project* **196**, 6–23.
- OLIVER, G. J. H., CORFU, F. & KROGH, T. E. 1993. U–Pb ages from SW Poland: evidence for a Caledonian suture between Baltica and Gondwana. *Journal of the Geological Society, London* **150**, 355–69.
- PEDERSEN, R.-B., FURNES, H. & DUNNING, G. R. 1991. A U/Pb age for the Sulitjelma Gabbro, North Norway: further evidence for the development of a Caledonian marginal basin in Ashgill–Llandovery times. *Geological Magazine* **128**, 141–53.
- ROEDER, P. L., MCARTHUR, D., MA, X.-P., PALMER, G. R. & MARIANO, A. N. 1987. Cathodoluminescence and microprobe study of rare-earth elements in apatite. *American Mineralogist* **72**, 801–11.
- ROSS, C. S. & SHANNON, E. V. 1926. The minerals of bentonites and related clays and their physical properties. *American Ceramic Society Journal* **9**, 77–96.
- SOPER, N. J., STRACHAN, R. A., HOLDSWORTH, R. E., GAYER, R. A. & GREILING, R. O. 1992. Sinistral transpression and the Silurian closure of Iapetus. *Journal of the Geological Society, London* **149**, 871–80.
- SRODON, J. 1980. Precise identification of illite/smectite interstratification by x-ray powder diffraction. *Clays and Clay Minerals* **28**, 401–11.
- TRENCH, A. & TORSVIK, T. H. 1992. The closure of Iapetus Ocean and Tornquist Sea: new palaeomagnetic constraints. *Journal of the Geological Society, London* **149**, 867–70.
- VERNIERS, J. & VAN GROOTEL, G. 1991. Review of the Silurian in the Brabant Massif, Belgium. *Annales de la Société Géologique de Belgique* **114**, 163–93.
- WATSON, E. B. 1979. Zircon saturation in felsic liquids: experimental results and applications to trace-element geochemistry. *Contributions to Mineralogy and Petrology* **70**, 407–19.
- WATSON, E. B. & GREEN, T. H. 1981. Apatite/liquid partition coefficient for the rare-earth elements and strontium. *Earth and Planetary Science Letters* **56**, 405–21.
- WILLIAMS, D. M., O'CONNOR, P. D. & MENUGE, J. 1992. Silurian turbidite provenance and the closure of Iapetus. *Journal of the Geological Society, London* **149**, 349–57.
- WILSON, M. 1989. *Igneous Petrogenesis*. London: Chapman and Hall, 466 pp.
- WRAY, D. S. 1995. Origin of clay-rich beds in Turonian chalks from Lower Saxony, Germany — a rare-earth element study. *Chemical Geology* **119**, 161–73.
- WRIGHT, J., SCHRADER, H. & HOLSER, W. T. 1987. Paleoredox variations in ancient oceans recorded by rare-earth elements in fossil apatite. *Geochimica et Cosmochimica Acta* **51**, 631–44.